

# Non-hermitean delocalization in an array of wells with variable-range widths

V.G.Benza

Facolta' di Scienze, Universita' dell'Insubria  
Via Lucini 3, 22100 Como  
also INFM, unita' di Milano,  
Via Celoria 16,20133 Milano

November 11, 2019

## Abstract

Nonhermitean hamiltonians of convection-diffusion type occur in the description of vortex motion in the presence of a tilted magnetic field as well as in models of driven population dynamics. We study such hamiltonians in the case of rectangular barriers of variable size. We determine Lyapunov exponent and wavenumber of the eigenfunctions within an adiabatic approach, allowing to reduce the original  $d=2$  phase space to a  $d=1$  attractor.  
PACS numbers:05.70.Ln,72.15Rn,74.60.Ge

## 1 Introduction

Quantum mechanics in an imaginary magnetic field (IMF) has been studied by various authors, after Hatano and Nelson [1] pointed out its relevance in describing the competition between drift and pinning for a vortex in the presence of columnar defects. The kinetic part of the hamiltonian with IMF is a convection-diffusion operator; operators of this type occur as well in models of driven population dynamics [2], [3], [4]. Due to the convection term, parity is violated and the wave function is exponentially magnified along a given direction; as a consequence, it can keep a localized character provided its decay, generated by the disordered potential, wins over the IMF amplification. In the zero-IMF reference hamiltonian the decay, if disorder does not violate parity, is characterized by the inverse of a single localization length on both sides. With convection, when the decay is exactly compensated by the IMF magnification factor, the wave function becomes delocalized. The spectrum at the critical point bifurcates, and is distributed along a  $d=1$  curve in the complex plane. This scenario was proved to be valid with various potential distributions (gaussian, box, Cauchy); it has been confirmed for lattice models with disordered hopping [5], [6], [7], [8], [9], [10]. In the hermitean case, one can turn the eigenvalue problem into a Langevin equation, and determine the spectral properties [11] from the steady state distribution of the

Langevin problem. Here we generalize this approach to complex-valued stochastic equations, as needed when dealing with non-hermitean hamiltonians. Rather than starting with a gaussian  $\delta$ -correlated potential, which would lead to a Langevin equation, we consider a piecewise constant potential  $V(x)$ , a model originally studied by Benderskii and Pastur [12] in the hermitean case. The reasons for our choice will become clear in the sequel. If, e.g.,  $V(x) = V_0, V_1$  with  $V_0 = 0$  and  $V_1 < 0$ ,  $V(x)$  describes equally engineered trapping defects in an homogeneous medium. We assume that free segments and trapping segments are independent random variables, with fixed average length  $l_0, l_1$  respectively. Although the stochastic equation is no longer of Langevin type, the probability distribution still satisfies a differential equation. This equation allows for an adiabatic approach, which would be impossible with white noise. We can thus reduce the phase space to a one-dimensional attractor  $\mathcal{L}$ , strongly simplifying the search for steady state. The “dynamic variable” of the stochastic equation is the logarithmic derivative  $z(x)$  of the wave function. From the mean value  $\langle z(E) \rangle$ , ( $E = E_r + i \cdot E_i$ ) one extracts the degree of exponential growth of the wave function, i.e. the inverse of the localization length, as well as a wavenumber. Generically we find that the localization length decreases when  $E$  departs from the real axis, and increases with  $E_r$ : the latter behavior is consistent with a known property of  $z(E)$  in the hermitean case. In the presence of an IMF, the bifurcation of the spectrum at a critical value of  $E_r$ , from the real axis to the complex plane, can be easily recovered from such properties. The level lines of the surface  $\langle z_r(E) \rangle$  determine the complex branches of the spectrum, corresponding to extended solutions. Three different regimes (low, high and intermediate  $E_r$ ) will be analyzed in the next three sections.

## 2 Langevin formulation of the quantum eigenvalue problem

The eigenvalue problem  $\hat{H}\psi = E \cdot \psi$  for a d=1 Hamiltonian  $\hat{H}_0 = -\frac{d^2}{dx^2} + V(x)$  with disordered potential  $V(x)$  translates into a Langevin equation for the logarithmic derivative  $z$  of the wave function  $\psi$ :

$$\frac{dz}{dx} = -(z^2 + E) + V(x); \quad z = \frac{\psi'}{\psi}. \quad (1)$$

As it is well known, one can limit the analysis to real-valued wave functions. The deterministic part of the equation is invariant under space inversion ( $z(-x) = -z(x)$ ) ; hence, if the statistical properties of  $V(x)$  are also invariant, the backward and forward  $x$ -evolution of  $z$  are equivalent, i.e. they approach the same steady state. One defines the Lyapunov exponent  $\gamma(E)$ :

$$\begin{aligned} \gamma(E) &= \lim_{x \rightarrow \infty} \frac{\langle \ln r(x) \rangle}{x} \\ r^2(x) &= \psi^2(x) + \psi'^2(x) \end{aligned}$$

where the average is over  $V(x)$ ;  $\gamma(E)$  is always positive for disordered potentials with rapidly decaying correlations [14]. The following identity is shown to hold:

$$\gamma(E) = \langle z \rangle \quad (2)$$

The Lyapunov exponent gives the exponential growth rate of the wave function ( $\psi(x) \approx \exp[\pm\gamma \cdot x]$   $x \rightarrow +\infty$ ): here, by Oseledec's theorem, the plus sign always occurs, but for a single case, corresponding to the physical (square-summable) solution [13]. Consistently, one has indeed  $\langle z \rangle > 0$  and a non-even steady state distribution  $P(z)$ . Let us now examine how this picture is changed upon adding an external (constant) imaginary magnetic field (IMF). In the hamiltonian, this is mimicked by:  $\hat{H} = -(\frac{d}{dx} - a)^2 + V(x)$ , implying  $z \rightarrow z - a$  in Eq. 1. The space-inversion invariance is broken by the convection term  $a \cdot \frac{d}{dx}$  and different exponential growth rates are found at  $x \rightarrow +\infty$  and  $x \rightarrow -\infty$ . On qualitative grounds, the asymptotic behavior is  $\psi(\pm L) \approx \exp[(\pm \cdot a - \langle z_r(E) \rangle) \cdot L]$  ( $L \gg 1$ ) and the solution delocalizes when  $\langle z_r(E) \rangle - a = 0$ .

Alternatively one can gauge away the IMF from the Schrodinger equation, thus restoring Eq. 1, but with new boundary conditions: e.g., in the case of a double-sided problem, from  $\psi(-L) = \alpha_-$ ,  $\psi(L) = \alpha_+$ , one gets  $\psi(-L) = \exp(a \cdot L) \cdot \alpha_-$ ,  $\psi(L) = \exp(-a \cdot L) \cdot \alpha_+$ . Here we study Eq. 1 with complex  $E = E_r + i \cdot E_i$ , and look for the steady state distribution  $P(z) = P(z_r, z_i)$  with  $z = z_r + i \cdot z_i$ . According to the previous arguments, delocalized solutions, if any, must lie on the level lines of the surface  $\langle z_r(E) \rangle$ ; such solutions are further characterized by a well defined wavenumber  $\langle z_i(E) \rangle$ . In the search for steady state, we adopt an adiabatic approach. This is possible with our model potential, due to a property of Eq. 1 with  $V(x) = 0$ . Let us discuss this property first. Equation 1 has two time-independent solutions (respectively stable and unstable critical point). If we denote with  $\epsilon = \epsilon_r + i \cdot \epsilon_i$  one of the square roots of  $E$ , the critical points are  $z_s = \epsilon_r - i \cdot \epsilon_r$  and  $z_u = -\epsilon_r + i \cdot \epsilon_r$  (the suffixes  $s, u$  meaning stable and unstable respectively, with  $\epsilon_i > 0$ ). The mentioned property is that the orbits satisfy the exact relation:

$$\begin{aligned} \frac{|z(x)|^2}{|\epsilon|^2} &= \frac{Ch(2B) - \cos(2A)}{Ch(2B) + \cos(2A)} \\ A &= \epsilon_r \cdot (x - x_0) + \gamma_r \\ B &= \epsilon_i \cdot (x - x_0) + \gamma_i \end{aligned} \quad (3)$$

where  $\gamma_r$  and  $\gamma_i$  are constants. As a model potential, we take  $V(x)$  two-valued, piecewise constant,  $V(x) = (V_0, V_1)$ ; the lengths of the  $V_l$  intervals are two independent random variables with distributions  $Q_l(x) = \frac{1}{c_l} \cdot \exp(-c_l \cdot x)$ , ( $l_l = \frac{1}{c_l}$ ). In order to write the analog of equation 1, we first introduce an independent stochastic variable  $s(x)$ , which assumes the values 0, 1 with distributions  $Q_0(x)$ ,  $Q_1(x)$ . The components  $P_0(x)$ ,  $P_1(x)$  of the probability of  $s(x)$  satisfy the rate equation:

$$\begin{aligned} \frac{dP_0}{dx} &= c_1 \cdot P_1 - c_0 \cdot P_0 \\ \frac{dP_1}{dx} &= c_0 \cdot P_0 - c_1 \cdot P_1, \end{aligned} \quad (4)$$

since  $s(x)$  stays on the  $l$ -th channel an average “time”  $\frac{1}{c_l}$ . The equation we looked for is then:

$$\frac{dz}{dx} = -(z^2 + E) + V_0 + s(x) \cdot (V_1 - V_0), \quad (5)$$

and, in components:

$$\begin{aligned} \frac{dz_r}{dx} &= -z_r^2 + z_i^2 - E_r + V_0 + s(x) \cdot (V_1 - V_0) \\ \frac{dz_i}{dx} &= -2 \cdot z_r \cdot z_i - E_i \end{aligned} \quad (6)$$

As it is well known, from Eq.1, if  $V(x)$  is gaussian, one gets a Fokker-Plank equation for the probability. Eq. 5 is no longer of Langevin type, but one can show that the probability distribution still satisfies a differential equation. The details of the derivation can be found in Ref. [14] and in the original paper [12]. In terms of the components  $P(s, z; x) = P_0(z, x), P_1(z, x)$ ;  $(P_0(z; x) = P(s=0, z; x), P_1(z; x) = P(s=1, z; x)$  one has:

$$\begin{aligned} \frac{dP_0}{dx} &= \left( -\frac{d}{dz_r} F_r^{(0)} - \frac{d}{dz_i} F_i^{(0)} \right) P_0 + c_1 \cdot P_1 - c_0 \cdot P_0 \\ \frac{dP_1}{dx} &= \left( -\frac{d}{dz_r} F_r^{(1)} - \frac{d}{dz_i} F_i^{(1)} \right) P_0 - c_1 \cdot P_1 + c_0 \cdot P_0 \\ F_r^{(0)} &= -z_r^2 + z_i^2 - E_r + V_0 \\ F_r^{(1)} &= -z_r^2 + z_i^2 - E_r + V_1 \\ F_i^{(0)} &= F_i^{(1)} = -2 \cdot z_r \cdot z_i - E_i \end{aligned} \quad (7)$$

We finally state our adiabatic approximation. We assume that the coefficients  $c_0$  and  $c_1$  are very small with respect to the characteristic “frequencies” of the two deterministic evolutions  $z^{(0)}(x)$  and  $z^{(1)}(x)$ , respectively associated with  $E^{(0)} = E_r - V_0 + i \cdot E_i$  and  $E^{(1)} = E_r - V_1 + i \cdot E_i$ . Such frequencies, as one easily realizes, are the square roots  $\epsilon^{(0)}, \epsilon^{(1)}$  of  $E^{(0)}$  and  $E^{(1)}$ .

### 3 Low energy case

We first examine the low  $E_r$  case. In both deterministic systems we assume  $|\epsilon_r| < |\epsilon_i|$ . This regime is out of the physical region since it implies  $E_r < V_l$ , ( $l = 0, 1$ ); in spite of that, its analysis will be found to be useful in the sequel. Upon averaging Eq. 3 over the variable  $B$ , which is fastly varying with respect to  $A$  when  $|\epsilon_r| < |\epsilon_i|$ , the factor  $\frac{Ch(2B) - \cos(2A)}{Ch(2B) + \cos(2A)}$  reduces to unity, and we get:

$$|z^{(l)}|^2 = |\epsilon^{(l)}|^2, \quad (l = 0, 1) \quad (8)$$

Each channel has a (metastable) attractor of circular shape, and the stochastic motion reduces to hops between such concentric orbits. One can get a picture of the single channel deterministic dynamics from Figs.1 and 2, where we show the vector field and

the probability distribution for Eq. 5 when  $s(x)$  is kept constant. We now proceed to determine the steady state of Eq. 7. We first eliminate the  $z_i$ -dependence from  $F_r^{(0)}$  and  $F_r^{(1)}$  by means of Eq. 8, then average over  $z_i$ , and obtain:

$$\begin{aligned}\frac{d}{dz_r}(-2 \cdot z_r^2 + 2 \cdot (\epsilon_i^{(0)})^2)P_0 &= c_1 \cdot P_1 - c_0 \cdot P_0 \\ \frac{d}{dz_r}(-2 \cdot z_r^2 + 2 \cdot (\epsilon_i^{(1)})^2)P_1 &= -c_1 \cdot P_1 + c_0 \cdot P_0.\end{aligned}\quad (9)$$

Here  $P_0 = P_0(z_r)$ ,  $P_1 = P_1(z_r)$ , are the components of the probability distribution averaged over  $z_i$ . The sum of the two equations gives:

$$(2 \cdot z_r^2 - 2 \cdot (\epsilon_i^{(0)})^2)P_0 + (2 \cdot z_r^2 - 2 \cdot (\epsilon_i^{(1)})^2)P_1 = K, \quad (10)$$

where  $K$  is a constant. It is readily verified that only with  $K = 0$  the positivity of the  $P$ 's is preserved. When  $|z_r|$  is large enough the flow is in the negative  $z_r$  direction on both channels; it turns positive for  $|z_r| < |\epsilon_i^{(l)}|$  ( $l = 0, 1$ ) respectively. Let us assume, without loss of generality,  $0 < \epsilon_i^{(1)} < \epsilon_i^{(0)}$ . It is readily verified that the particle gets trapped, on the  $z_r$  axis, within the stable critical points of the two channels, while the probability must be zero outside. Notice that upon including an indeterminacy in the radii we would get a non zero probability flow. Apart from the normalization factor  $H$ , the solutions have the form:

$$\begin{aligned}P_0(z_r) &= H^{-1} \frac{1}{|z_r^2 - (\epsilon_i^{(0)})^2|} \cdot \psi(z_r) \\ P_1(z_r) &= H^{-1} \frac{1}{|z_r^2 - (\epsilon_i^{(1)})^2|} \cdot \psi(z_r) \\ \psi(z_r) &= \left[ \left| \frac{z_r - \epsilon_i^{(0)}}{z_r - \epsilon_i^{(0)}} \right| \right]^{\mu_0} \cdot \left[ \left| \frac{z_r - \epsilon_i^{(1)}}{z_r - \epsilon_i^{(1)}} \right| \right]^{\mu_1} \\ \mu_l &= \frac{c_l}{4 \cdot \epsilon_i^{(l)}}\end{aligned}\quad (11)$$

The function  $P_l$  has an integrable power law singularity at the  $l$ -th channel's stable point, and a zero at the opposite channel's stable point. If we denote with  $p_0$  and  $p_1$  the integrals of  $P_0(z_r)$  and  $P_1(z_r)$ , they must satisfy the global equilibrium condition:

$$c_0 \cdot p_0 = c_1 \cdot p_1. \quad (12)$$

We determined the solution in the region  $c_0 + c_1 = 1$  under this condition. The power exponent of the distribution is a function of the ratio  $\frac{c_0}{c_1}$ , i.e. it is shaped by the average “residence times” over the two channels. The mean value  $\langle z_r \rangle$  is increasing with the ratio  $\rho = \frac{\epsilon_i^{(0)}}{\epsilon_i^{(1)}}$ , as shown in Fig.5. Since larger ratios imply larger values of  $|V_0 - V_1|$ , this simply means that the Lyapunov exponent increases with disorder, as it should be. As anticipated, the density of states must be zero in this regime. Our probability distribution, identically zero out of a given interval, is consistent with that: in fact, since the “particle” eventually belongs to such interval, any boundary condition  $z_r(L) = \bar{z}_L$  outside it cannot be fulfilled.

## 4 High energy case

We analyze now the regime  $E_r \gg 0$ , which corresponds to the condition  $|\epsilon_i| < |\epsilon_r|$  for both channels. Contrary to the former case, in Eq. 3 the variable A is now fastly varying with respect to B. The average over A gives:

$$\frac{|z|^2}{|\epsilon|^2} = -1 + \frac{|z|^2 + |\epsilon|^2}{|\epsilon_r \cdot z_i - \epsilon_i \cdot z_r|}, \quad (13)$$

wherefrom:

$$|\epsilon|^2 = |\epsilon_r \cdot z_i - \epsilon_i \cdot z_r|. \quad (14)$$

For each channel, the metastable attractor is made of a couple of parallel lines; each critical point (stable and unstable) belongs to one of them. The lines are orthogonal to the segment connecting the critical points. To sum up, in going from the low to the high energy limit, the attractor undergoes dilatation in the direction of such lines; this effect can be already seen in Fig.2, referring to the low energy regime. An indeterminacy arises, about which line is currently occupied by the “particle”:

$$z_i = \frac{\epsilon_i}{\epsilon_r} \cdot z_r \pm \frac{|\epsilon|^2}{\epsilon_r} \quad (15)$$

In Figs.3 and 4 we display the vector field and the probability distribution for Eq. 5 in the deterministic case (single channel), together with the attractor. For the total system we have the union of two couples of parallel lines, with distinct slopes. We proceed with our strategy, based on averaging Eq. 7 over  $z_i$ . Upon writing  $F_r^{(l)}$ , ( $l = 0, 1$ ) by means of Eq. 15 we have:

$$F_r = -z_r^2 + \left(\frac{\epsilon_i}{\epsilon_r} \cdot z_r\right)^2 \pm 2 \cdot \epsilon_i \cdot z_r + (\epsilon_i)^2, \quad (16)$$

where the dependence on  $E$  and  $V_l$  is written in terms of  $\epsilon$  and the following approximation is made:

$$z_i = \frac{\epsilon_i}{\epsilon_r} \cdot z_r \pm \left(\epsilon_r + \frac{(\epsilon_i)^2}{\epsilon_r}\right) \approx \frac{\epsilon_i}{\epsilon_r} \cdot z_r \pm \epsilon_r. \quad (17)$$

The force  $F^{(l)}(z_r)$  ( $l = 0, 1$ ) is split in a deterministic part and a fluctuating part, the latter being of order  $2 \cdot \epsilon_i^{(l)} \cdot z_r$ . This corresponds to a stochastic equation of the form:

$$\frac{dz_r}{dx} = -z_r^2 + \left(\frac{\epsilon_i}{\epsilon_r} \cdot z_r\right)^2 + (\epsilon_i)^2 + 2 \cdot \epsilon_i \cdot z_r \cdot \eta(x), \quad (18)$$

where  $\eta(x)$  is a white noise. We are then led to the Fokker-Plank equation:

$$\begin{aligned} \frac{dP_0}{dx} &= \frac{d}{dz_r} \left( -A^{(0)} + \frac{d}{dz_r} B^{(0)} \right) P_0 + c_1 \cdot P_1 - c_0 \cdot P_0 \\ \frac{dP_1}{dx} &= \frac{d}{dz_r} \left( -A^{(1)} + \frac{d}{dz_r} B^{(1)} \right) P_1 - c_1 \cdot P_1 + c_0 \cdot P_0 \\ A^{(l)} &= -(\alpha_l \cdot z_r)^2 + (\epsilon_i^{(l)})^2 \\ B^{(l)} &= D \cdot (\epsilon_i^{(l)})^2 \cdot [(z_r)^2 + (\xi^{(l)})^2] \\ \alpha_l^2 &= 1 - \left(\frac{\epsilon_i}{\epsilon_r}\right)^2 \end{aligned} \quad (19)$$

where  $D$  is the white noise coefficient and  $\xi^{(l)}$  is a regularizing parameter (the criteria used in fixing this parameter are illustrated in the caption of Fig.6). We evaluated numerically, by a perturbative procedure, the steady state solution of Eq. 19. To simplify things, we assumed  $c_0 = c_1 = c < 1$ . When the channels are uncoupled ( $c = 0$ ), the problem can be explicitly solved along the lines of the hermitean case (see, e.g., Ref. [11]). The two equations reduce to the form:  $\mathcal{M}^{(l)} P_l = \frac{d}{dz_r} J_l(z_r) = 0$ , where, with obvious notation,  $\mathcal{M}^{(l)}$  is the second order operator acting on  $P_l$ . The solutions correspond to a constant probability current  $J_l$  and here look like:

$$\begin{aligned} P_l(z_r) &= \frac{J_l}{B_l(z_r)} \int_{-\infty}^{z_r} dz' \exp[U_l(z_r) - U_l(z')] \\ U_l(z) &= (1/D) \left[ \frac{(1 + \alpha_l^2)}{\epsilon_i^l} \cdot \text{artg}\left(\frac{z}{\alpha_l}\right) - \frac{\alpha_l^2}{(\epsilon_i^{(l)})^2} \cdot z \right]. \end{aligned} \quad (20)$$

Upon substituting the series expansion  $P_l = \sum_k c^k \cdot P_l^{(k)}$ , ( $l = 0, 1$ ) in Eq. 19, one obtains an inhomogeneous equation for  $P_l^{(k+1)}$ , where  $P_l^{(k)}$  is the source term. The operator  $\mathcal{M}^{(l)}$  is easily inverted, with two integrals over  $z_r$ . This is performed numerically. In order to check for convergence, the area difference between successive approximants  $P_l^n = \sum_k^n c^k \cdot P_l^{(k)}$  is computed. In the cases exhibited here, we put  $c = 0.1$ , and find good convergence for  $n > 20$ . From the probability distribution  $P_l(z)$  we then get  $\langle z_r \rangle = \langle z_r \rangle_0 + \langle z_r \rangle_1$ , with obvious notation. In Fig.6 we plot the result  $\langle z_r \rangle$  as a function of  $E_r$ . The asymptotic behavior in the hermitean case is known:  $\langle z_r \rangle \approx (E_r)^{-2}$ , ( $E_i = 0$ )  $E_r > 1$  [14]. Our estimate, with  $E_i = 10$ , and  $E_r$  in the range: 50.  $< E_r < 120.$ , is of a much slower decay; further work is needed to clarify this point. When  $E_r$  is fixed,  $\langle z_r \rangle$  increases with  $|E_i|$ , as shown in Fig.7; we get  $\langle z_r \rangle \approx |E_i|^\beta$ ,  $\beta \approx 2$  for large enough  $|E_i|$ . A wavenumber  $\langle z_i(E) \rangle$  emerges as a further character of the solution: its value can be roughly estimated from  $\langle z_r \rangle$  and Eq. 15, where the sign ambiguity should be solved in favor of the line including the stable point. In the discrete case, the occurrence of a winding number was already pointed out in Ref. [4]. The wavenumber is to be associated with the physical solutions, which, out of the  $E_r$  axis, lie on the curve  $\langle z_r(E) \rangle = a$ . It is easily verified that  $\langle z_i(E) \rangle$  is an odd function of  $E_i$  while  $\langle z_r(E) \rangle$  is even; complex conjugate eigenvalues carry opposite wavenumbers. In the hermitean case the two eigenvalues merge, and the wavenumber, being a byproduct of broken parity, is zero for standing waves.

## 5 Intermediate energies

So far we studied two extreme cases, but intermediate energies in strong disorder can as well be treated; let us consider the following regime:  $V_1 \ll E_r \ll V_0$ . In this case the deterministic solutions satisfy Eqs. 8 and 14 respectively, i.e. channel (0) is in a “low energy” regime, and channel (1) in a “high energy” one. The metastable attractor  $\mathcal{L}$  is made up of a circle plus a couple of parallel lines. The system for  $P_0$  and  $P_1$  is an hybrid between Eqs. 9 and 19. In this case the first order operator of Eq.

9 is coupled with the second order one of Eq. 19: this makes an iterative procedure hardly convergent. Consistently with results from direct numerical integration of Eq. 5, we assign an indeterminacy  $\delta$  to the circular orbit:

$$\frac{|z|^2}{|\epsilon|^2} = 1 + \delta. \quad (21)$$

A spread in the circular attractor clearly appears in Fig.2, wherefrom an estimate for  $\delta$  can be extracted [15]. After this, the steady state equation involves two second order operators:

$$\begin{aligned} \frac{d}{dz_r} [F_r^{(0)} - \frac{d}{dz_r} \mathcal{D}^0] P_0 &= c_1 \cdot P_1 - c_0 \cdot P_0 \\ \frac{d}{dz_r} [A^{(1)} - \frac{d}{dz_r} B^{(1)}] P_1 &= -c_1 \cdot P_1 + c_0 \cdot P_0 \\ \mathcal{D}^0 &= (\delta \cdot |\epsilon^0|^2)^2 \end{aligned} \quad (22)$$

We proceed along the lines of the previous section, i.e., by an iterative perturbation scheme. At uncoupled channels ( $c = 0$ ) the “low energy” equation coincides now with the well-known one ([11]), holding in the hermitean case. Its solution carries a non zero probability current: in the present context, it comes from the spread of the circular attractor. The “high energy” integral was already exhibited in the previous section. In Fig.9 we show our result, the surface  $\langle z_r(E) \rangle$ . The corresponding plot in the high energy regime is reported for comparison in Fig.8; its level lines in the  $E$  plane are shown in Fig.10. Qualitative agreement is found with previous numerical and analytical results. An estimate of  $\langle z_i(E) \rangle$  can be derived from the adiabatic equations 15 and 8.

## 6 Conclusions

We studied nonhermitean delocalization in the presence of disordered potentials of Kronig-Penney type, where the barriers have random length. We translated the hamiltonian eigenvalue problem into a stochastic equation for the logarithmic derivative of the wave function ( $z = \frac{\psi'}{\psi}$ ). From the steady state distribution of  $z$  we determined the Lyapunov exponent. Our approach, valid under suitable adiabatic conditions, describes the steady state in terms of the real part of  $z$ . The imaginary part of  $\langle z \rangle$ , an effective wavenumber, can be recovered by means of the adiabatic formulae 8,15. We analyzed two regimes: a) intermediate energies ( $V_1 \ll E_r \ll V_0$ ); b) high energies ( $V_1, V_0 \ll E_r$ ). The behavior of the system in other regimes is currently under investigation [15]. In case (a), the particle hops in the  $z$  plane between a strip and a circle, the strip carrying a probability current. The circle, which acts as a trap for the particle, is absent in case (b), where the ‘particle’ hops between two strips, with different slopes. Two currents coalesce in this case. We obtained that  $\langle z_r \rangle$  is always decreasing with  $E_r$ : at higher energies the wave functions have larger localization length. At fixed  $\langle E_r \rangle$ ,  $\langle z_r \rangle$  increases with  $|E_I|$ : this means that dissipation (associated with  $E_i$ ) enhances the localization. The effective wavenumber

$\langle z_i \rangle$  increases with  $E_r$ , as one would expect with normal dispersion. Eigenvalues corresponding to extended functions must lie on the curve  $\langle z_r(E) \rangle - a = 0$ , where  $a$  is the convection coefficient. We finally add some comments on the density of states (DOS). Most analytical results on the DOS in the presence of an IMF, possibly with the single exception of the semiclassical analysis by Silvestrov [16], are concerned with the discrete case. Disorder averaging of the resolvent operator can indeed be performed in various discrete models, thus obtaining the DOS in explicit form [7],[8],[9],[10]. The Langevin approach gives the DOS for the hermitean hamiltonian in the continuum. As a preliminary step in that procedure, one writes the definition of the DOS in terms of the  $z$  variable: this simply amounts to requiring that  $z(x, E)$  must fulfill the boundary condition:  $z(L, E) = z_L$ . This condition is all is needed as long as the mapping from  $E$  to  $z(L, E)$  is invertible, which is precisely the case in the hermitean problem. Whether anything similar holds in the complex case is, as far as we know, an open question.

## References

- [1] N.Hatano,D.R.Nelson:Phys.Rev.Lett.**77**,570(1996).
- [2] J.Miller,Z.J.Wang:Phys.Rev.Lett.**76**,1461(1996).
- [3] J.D.Murray: Mathematical Biology, Springer, New York (1993).
- [4] D.R.Nelson,N.M.Shnerb:Phys.Rev.**E58**,1383 (1998).
- [5] N.Hatano,D.R.Nelson:Phys.Rev.**B56**,8651(1997).
- [6] N.Hatano,D.R.Nelson:Phys.Rev.**B58**,8384(1998).
- [7] P.W.Brouwer,P.G.Silvestrov,C.W.J.Beenakker:Phys.Rev.**56**,R4333(1997).
- [8] E.Brezin,A.Zee:Nucl.Phys.**B509**,(1998).
- [9] J.Feinberg,A.Zee:Nucl.Phys.**B504**,579(1997).
- [10] I.Y.Goldsheid,B.A.Khoruzenko:Phys.Rev.Lett.**80**, 2897(1998).
- [11] B.I.Halperin:Phys.Rev.**139**,A104(1965).

- [12] M.M.Benderskii,L.A.Pastur: JETP **57**,284(1969).
- [13] B.Souillard in:"Chance and Matter", J.Souletie,J.Vannimenus, R.Stora editors,North Holland,(1987).
- [14] I.M.Lifshits,S.A.Gredeskul,L.A.Pastur:"Introduction to the theory of disordered systems",Wiley,New York,(1988).
- [15] V.G.Benza,S.Manildo, in preparation.
- [16] P.G.Silvestrov:Phys.Rev.**58**,R10111(1998).

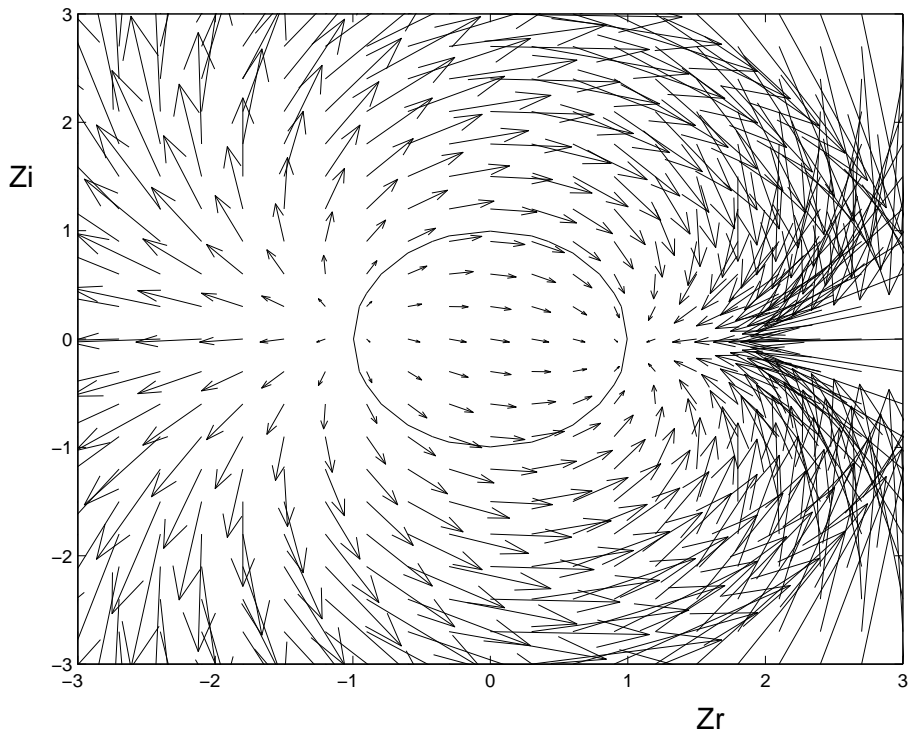


Fig.1:Vector field  $(F_r, F_i)$  in the  $z$  plane for the Equation 5 at fixed  $s(x)$  (deterministic), in the low energy regime. The variables  $z_r, z_i$  are in arbitrary units of  $(length)^{-1}$ . The superimposed circle corresponds to the metastable attractor discussed in the text (see Eq. 8). The two critical points characterized by the condition  $F_r = 0, F_i = 0$  belong to the circle.

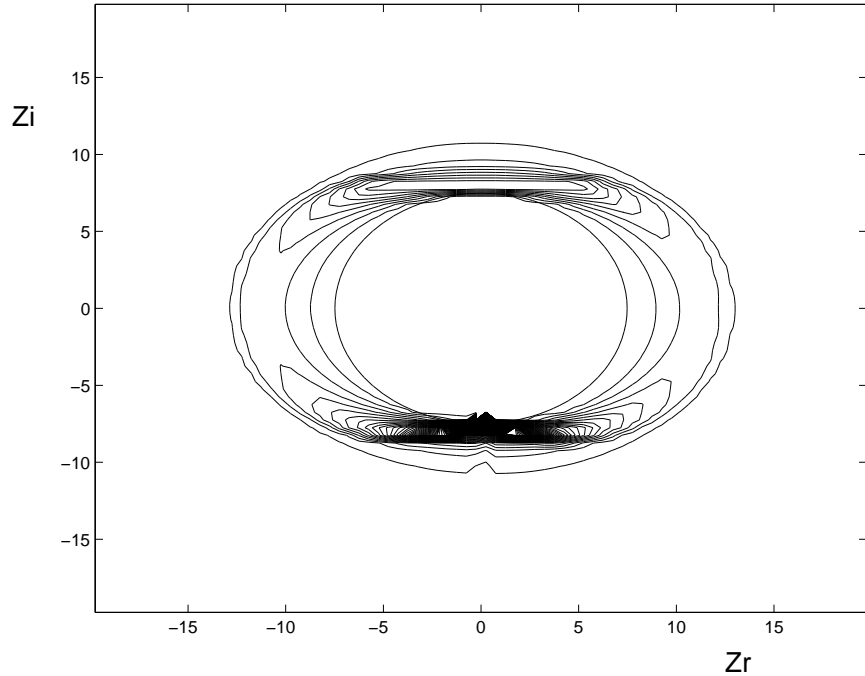


Fig.2: Numerical integration of the Equation 5 with  $s(x) = 0$  in the low energy regime: level lines of the probability distribution at an intermediate time. The variables  $z_r, z_i$  are in arbitrary units of  $(length)^{-1}$ . The distribution is obtained from 2000 random initial conditions. The inner circle is superimposed: it corresponds to the metastable attractor, as calculated from Eq. 8, with the values  $E_r - V_0 = -56, E_i = -1.35$  used in the numerical integration. The variables  $E_r, E_i$  are in arbitrary units of  $(length)^{-2}$ . The unstable critical point is in the upper part; in the lower part, the peak at the stable point can be seen. The distribution deviates from a purely circular behavior; it is elongated in the aequator direction, the critical points being the poles. In fact going from the low to the high energy regime (see Eq.15) the attractor is converted into a couple of lines. These lines are through the poles, and parallel to the aequator.

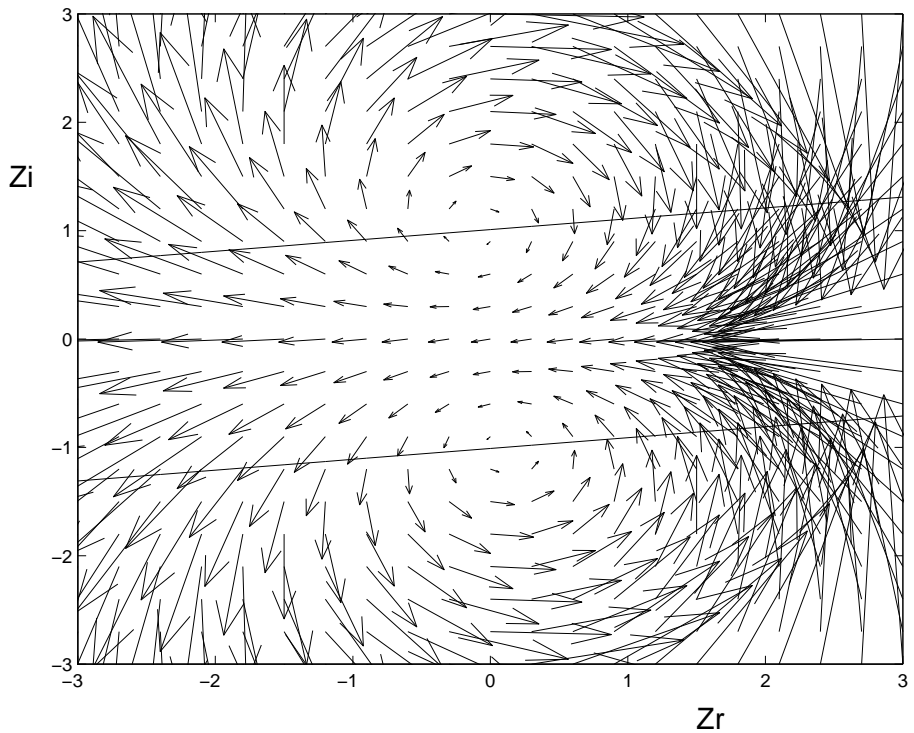


Fig.3:Vector field  $(F_r, F_i)$  of Equation 5 with fixed  $s(x)$  in the high energy regime. The variables  $z_r, z_i$  are in arbitrary units of  $(length)^{-1}$ . The two superimposed parallel lines through the critical points  $(F_r = 0, F_i = 0)$  correspond to the metastable attractor (see Eq. 15). The lines are orthogonal to the segment connecting the critical points.

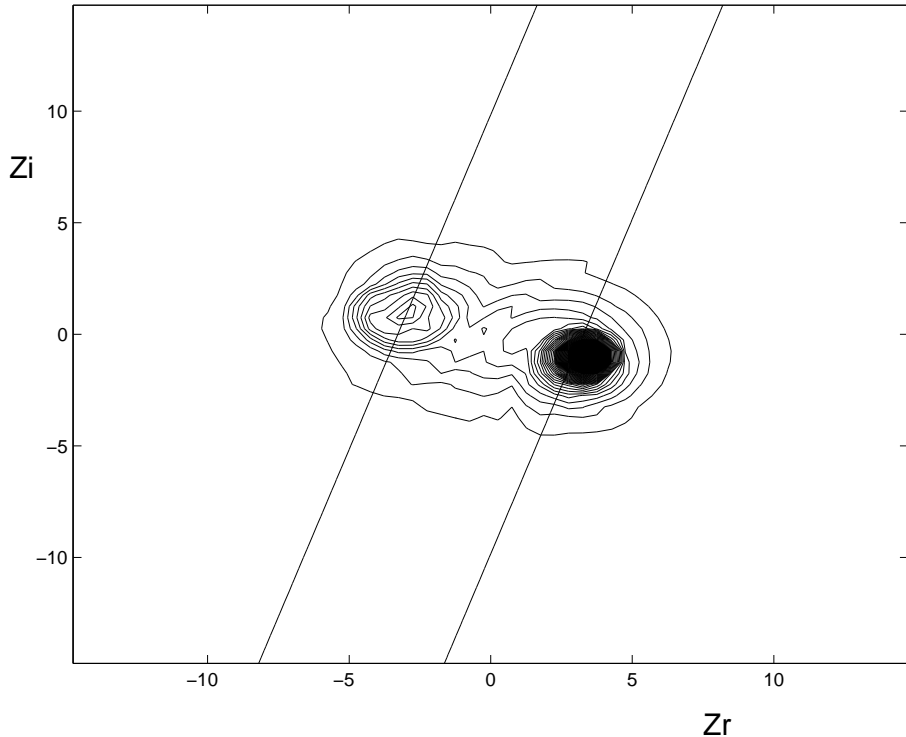


Fig.4: Numerical integration of Eq. 5 with  $s(x) = 1$  in the high energy regime (random initial conditions): level lines of the probability distribution at an intermediate time. The variables  $z_r, z_i$  are in arbitrary units of  $(length)^{-1}$ . The energy values are  $E_r - V_1 = 10.35, E_i = 7.5$ , in arbitrary units of  $(length)^{-2}$ . The unstable critical point is in the upper left. The metastable attractor (two parallel lines) has been superimposed. One can notice, in particular around the unstable point, that the distribution is slightly elongated in the direction of the attractor.

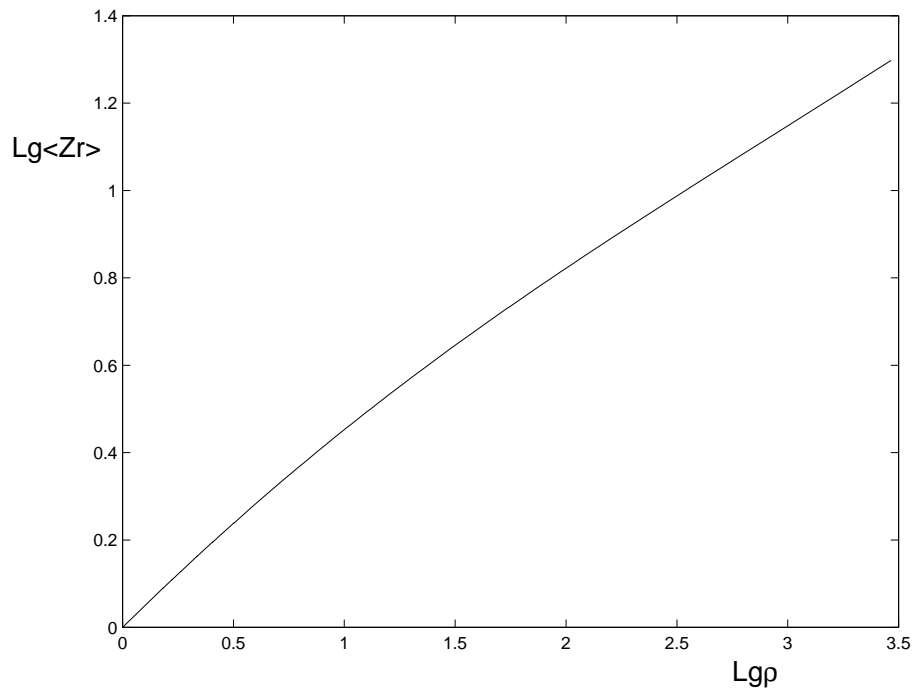


Fig.5: Low energy regime; from the solution (Eq. 11) of the steady state Equation 9 for the probability: log-log plot of  $\langle z_r \rangle$  versus  $\rho = \frac{\epsilon_i^{(0)}}{\epsilon_i^{(1)}}$ . Higher  $\rho$  means higher disorder (see text): the localization length decreases with  $\rho$ .

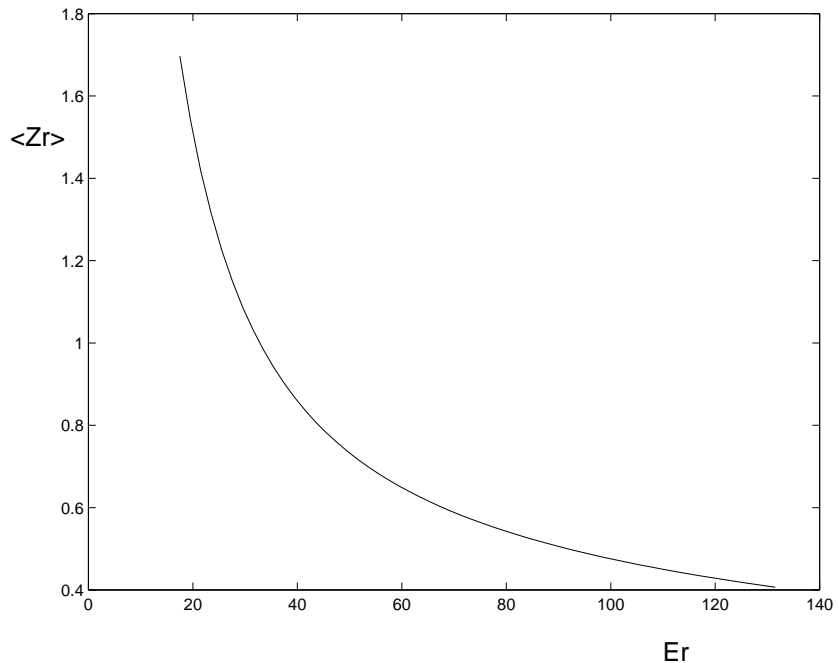


Fig.6: High energy regime:  $\langle z_r \rangle$  versus  $E_r$  at fixed  $E_i$ , ( $E_i = 10$ ). The variable  $z_r$  is in arbitrary units of  $(length)^{-1}$ , and  $E$  in arbitrary units of  $(length)^{-2}$ . The origin of the energy axis corresponds to  $E_r = \frac{1}{2} \cdot (V_{(0)} + V_{(1)})$ ;  $V_{(0)} - V_{(1)} = 5$ . From numerical integration of the probability Equation19 at steady state, with  $D = 0.1$ . The regularization parameter is:  $\xi^{(l)} = \epsilon_i^l$ . With this choice  $\xi^{(l)}$  has the same order of magnitude of  $z_r$  at the stationary points:  $z_r = \pm \epsilon_i^{(l)}$ .

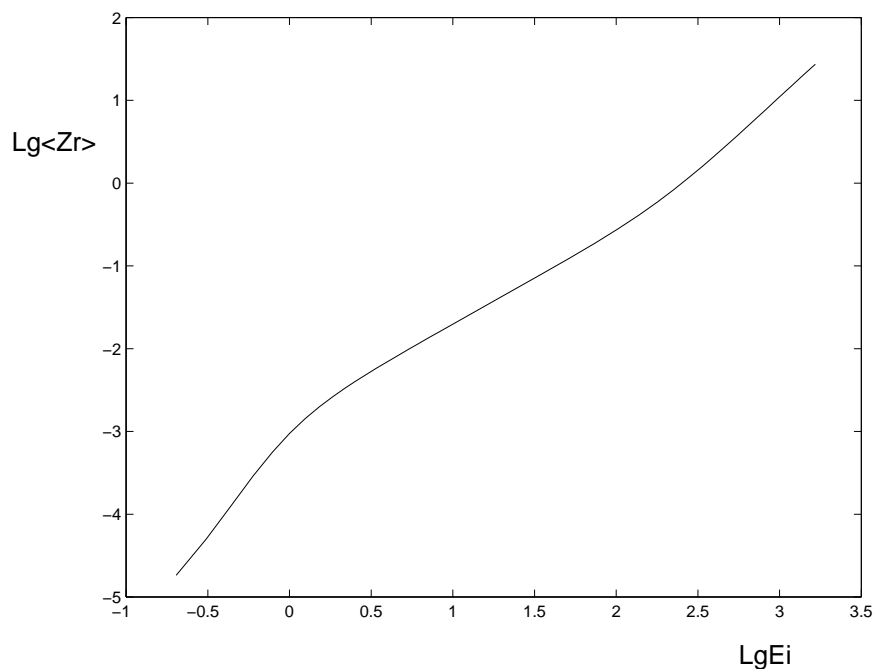


Fig.7: High energy regime: log-log plot of  $\langle z_r \rangle$  versus  $E_i$  at fixed  $E_r$ :  $E_r - V_{(1)} = 60.$ ,  $E_r - V_{(0)} = 30.$  Same Equation and parameters as in Fig.6.

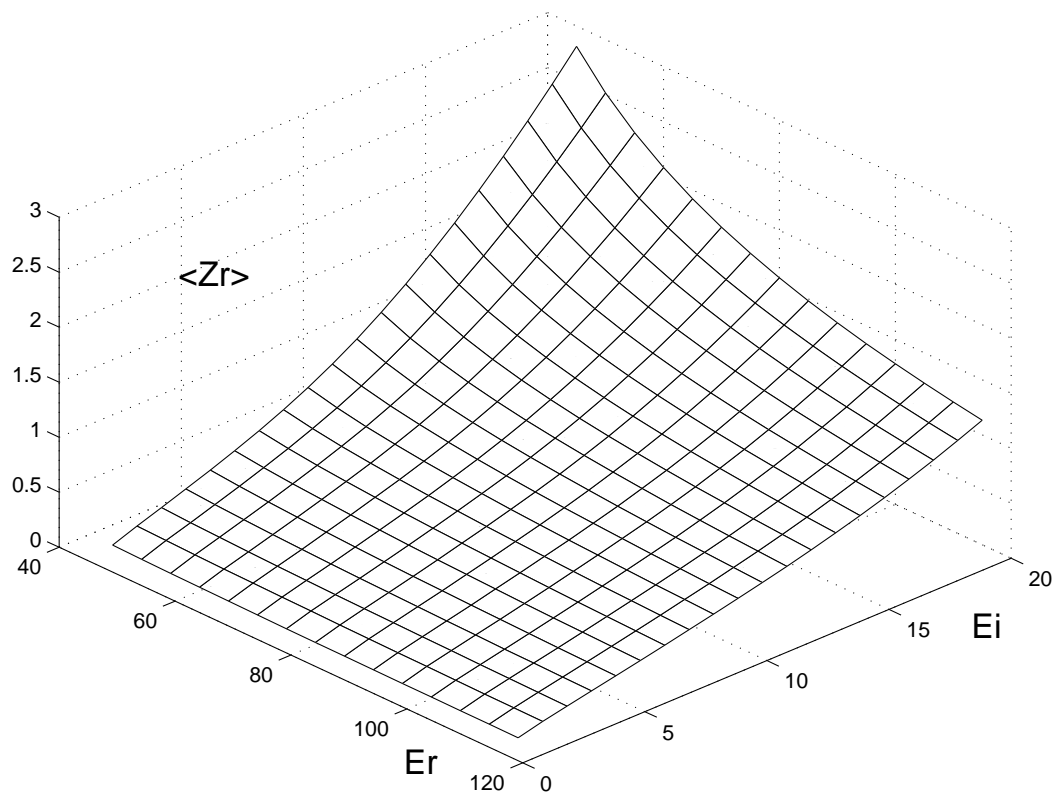


Fig.8: High energy regime:global behavior of  $\langle z_r \rangle$  versus  $E$ ;  $V_{(0)} - V_{(1)} = 30$ . The variable  $z_r$  is in arbitrary units of  $(length)^{-1}$ , and  $E$  in arbitrary units of  $(length)^{-2}$ . From numerical integration of the probability Equation 19. Same parameters as in Figs. 6,7.

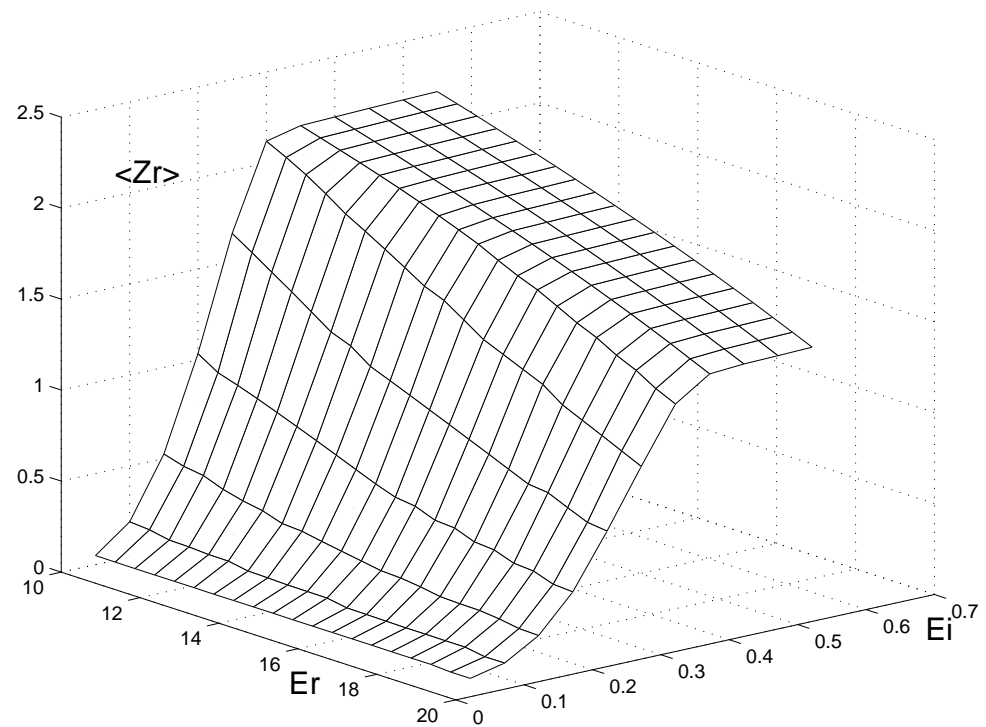


Fig.9: Intermediate energy regime, numerical integration of the probability Equation 22:  $\langle z_r \rangle$  versus  $E$ ,  $D = 0.1$ ,  $\delta = 25.$ ,  $V_{(0)} - V_{(1)} = 30$ . The variable  $z_r$  is in arbitrary units of  $(length)^{-1}$ , and  $E$  in arbitrary units of  $(length)^{-2}$ .

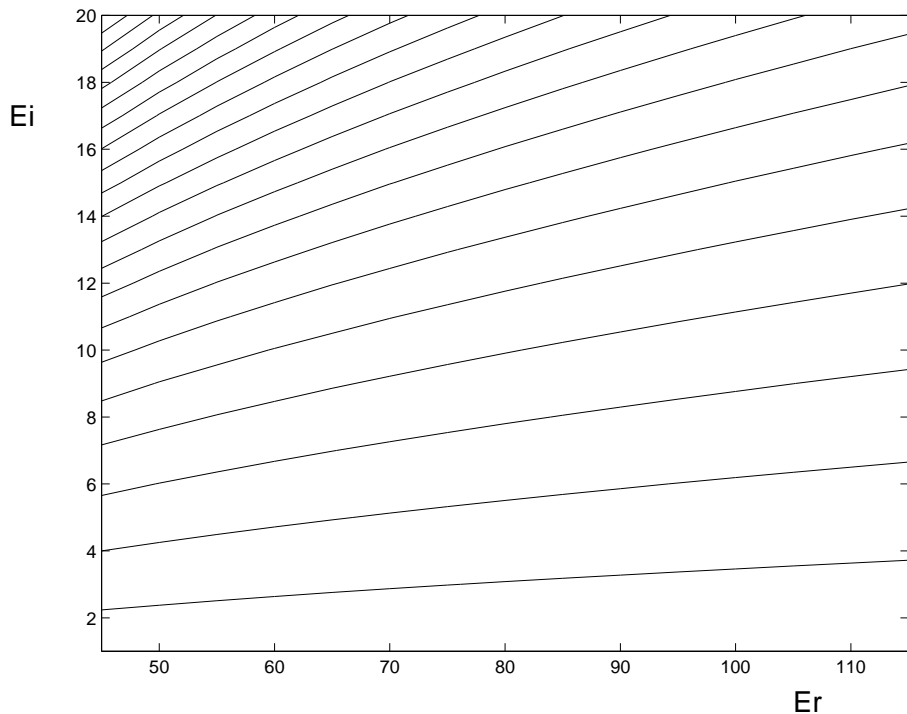


Fig.10: High energy regime. Level lines of the surface  $\langle z_r(E) \rangle$ ; same Equation and parameters as in Fig.8.  $E_r, E_i$  are in arbitrary units of  $(\text{length})^{-2}$ . Each line identifies a region of allowed eigenvalues, for a fixed convection parameter  $a$ :  $a$  increases from bottom right to top left.